Fragmentation and scales in nuclear giant resonances

W. D. Heiss*, R. G. Nazmitdinov† and F. D. Smit**

*National Institute for Theoretical Physics, Stellenbosch Institute for Advanced Study, and Institute of Theoretical Physics, University of Stellenbosch, 7602 Matieland, South Africa
†Department de Física, Universitat de les Illes Balears, E-07122 Palma de Mallorca, Spain and Bogoliubov Laboratory of Theoretical Physics, Joint Institute for Nuclear Research, 141980 Dubna, Russia
**iThemba LABS, PO Box 722, Somerset West 7129, South Africa

Abstract. We propose a general approach to characterise fluctuations of measured cross sections of nuclear giant resonances. Simulated cross sections are obtained from a particular, yet representative self-energy which contains all information about fragmentations. Using a wavelet analysis, we demonstrate the extraction of time scales of cascading decays into configurations of different complexity of the resonance. We argue that the spreading widths of collective excitations in nuclei are determined by the number of fragmentations as seen in the power spectrum. An analytic treatment of the wavelet analysis using a Fourier expansion of the cross section confirms this principle. A simple rule for the relative life times of states associated with hierarchies of different complexity is given.

Keywords: nuclear reactions, giant resonances
PACS: 24.30.Cz, 24.60.Ky, 24.10.Cn

INTRODUCTION

Nuclear Giant Resonances (GR) have been the subject of numerous investigations over several decades [1]. Some of the basic features such as centroids and collectivity (in terms of the sum rules) are reasonably well understood within microscopic models [2, 3]. However, the question of how a collective mode like the GR dissipates its energy is one of the central issues in nuclear structure physics.

According to accepted wisdom, GRs are essentially excited by an external field through a one-body interaction. It is natural to describe these states as collective 1p-1h states. Once excited, the GR progresses to a fully equilibrated system via direct particle emission and by coupling to more complicated configurations (2p-2h, 3p-3h, etc). The former mechanism gives rise to an escape width, while the latter yields spreading widths ($\Gamma^{\downarrow}$). An understanding of lifetime characteristics associated with the cascade of couplings and scales of fragmentations arising from this coupling (cf [4, 5, 6, 7]) remains a challenge. Recent high energy-resolution experiments of the Isoscalar Giant Quadrupole Resonance (QR) [8, 9, 10] provide new insights into this problem.

It has been shown by Shevchenko *et al.* [8] that the fine structure of the QR observed in (p, p') experiments is largely probe independent. Furthermore, a study of the fine structure using wavelet analysis [11, 12, 13] reveals energy scales [9, 10] in the widths of the fine structure displaying a seemingly systematic pattern, as can be seen in Figs.8

and 9 of Ref.[10]. The power spectrum patterns vary with the structure of the nucleus being studied. They are obtained by summing the wavelet coefficients (an integrated overlap of the mother wavelet and the excitation energy spectrum) onto the wavelet energy-scale axis. While the physical meaning of the results of such an analysis is still being debated, we try here to offer a general explanation. However, we do not embark on a specific microscopic analysis, but rather make use of general and well-established techniques of many-body theory. Gross effects due to nuclear deformation and coupling to the continuum [5] are not discussed; we rather focus on the decay of the QR into configurations of various complexity.

SELF-ENERGY AND CROSS SECTION

To proceed we use the Green's function approach. A central role is played by the self-energy whose finer structure is imparted upon the Green's function via the solution of Dyson's equation which reads [14]

$$G_{\alpha,\beta}(\omega) = G^0_{\alpha,\beta}(\omega)) + G^0_{\alpha,\gamma}(\omega)\Sigma_{\gamma,\gamma'}(\omega)G_{\gamma',\beta}(\omega) \tag{1}$$

which is solved by

$$G_{\alpha,\beta}(\omega) = ((G^0_{\alpha,\beta}(\omega))^{-1} - \Sigma_{\alpha,\beta}(\omega))^{-1}, \tag{2}$$

where we assume $G^0(\omega) = \delta_{\alpha,\beta}/(\omega - \varepsilon)$ to be diagonal in the basis $\alpha, \beta, \ldots$ while the complicated pole structure of $G(\omega)$ is generated by that of the self-energy $\Sigma_{\alpha,\beta}(\omega)$. The pole structure of G carries over to the scattering matrix given by

$$\begin{aligned} T_{\alpha,\beta}(\omega) &= \Sigma_{\alpha,\beta}(\omega) + \Sigma_{\alpha,\beta'}(\omega)G^0_{\beta',\alpha'}(\omega)T_{\alpha',\beta}(\omega) &(3)\\ &= \Sigma_{\alpha,\beta}(\omega) + \Sigma_{\alpha,\beta'}(\omega)G_{\beta',\alpha'}(\omega)\Sigma_{\alpha',\beta}(\omega) &(4)\end{aligned}$$

from which a cross section $\sim |T_{\alpha,\alpha}(\omega)|^2$ is obtained.

Within the excitation energy range of the QR the nucleus has a high density of complicated states of several tens of thousands per MeV and even more for heavy nuclei. These many states appear in the self-energy as poles in the complex energy plane close to the real axis. The small widths imply they are long-lived states and traditionally classed as compound states. The simpler intermediate structure of the excitation is expressed by the substantial fluctuations of the corresponding residues associated with the poles of the self-energy $\Sigma(\omega)$ [15]. In other words, while the individual pole positions of $\Sigma(\omega)$ are virtually unstructured [16], it is the variation of the corresponding residues that bears all the information about intermediate structure. Note that our approach differs from a traditional microscopic calculation in that from the outset we start from a random distribution of pole terms representing compound states. Traditional microscopic approaches cannot address such finer structures [17].

We assume that the QR, being a collective 1p-1h state, decays via a cascade progressing through (2p-2h)-, (3p-3h)-configurations and so forth to the eventual compound states. In turn, each of the intermediate states (including the initial QR) can either decay directly to the ground state or via some more complicated intermediate state. Below

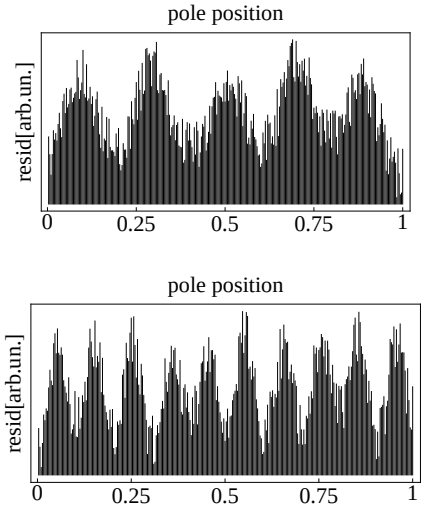

FIGURE 1. Schematic illustration of the residues of the self-energy: for 5 (top) and 10 (bottom) intermediate states. The heights of each of the 300 bars which are situated at the real parts of the poles of the self-energy illustrate the relative variation of the residues. The randomisation is clearly discernible.

we will show that it is this mixture that is seen in the cross section and extracted by wavelet analysis, and it is the variety and cascading complexity of states that invokes the structure of the residues of the poles of the self-energy. Of importance to note is that the number of states available within the energy domain of the QR increases with its complexity: for example, five (2p-2h)-states, ten (3p-3h)-states, down to several thousand compound states (the numbers six or eleven should be taken as examples without claim for quantitative correctness). Moreover, the corresponding life times are expected to increase in line with their increasing complexity, which is in accordance with their decreasing spreading widths (below we come back to this particular aspect of scaling).

As a typical case study we investigate here a wavelet analysis of a simulated cross section that results from a particular input for the self-energy. Since arbitrary units are used, we concentrate on the energy interval [0,1] and use for the pole position $\varepsilon = 0.5 - i0.5$ of the single pole of G_0 (see Eq.(2)). The number of compound states is assumed to be 300; this is of course much less than the experimental level density in the region of a QR for a medium or heavy nucleus, but it suffices for our demonstration. The real parts of the pole positions are assumed to be randomly distributed with a uniform distribution of the mean distance 1/300; the imaginary parts are randomly distributed in the interval [0.004,0.007].

For illustration we consider as a specific example four different sets of residues of the self-energy. The self-energy reads

$$\Sigma(\omega) = \sum_{k=1}^{300} \frac{r_k}{\omega - \omega_k} \tag{5}$$

where each residue r_k is the sum of four subsets; each subset is distributed by a Lorentzian with specific widths γ_i, $i = 1,\ldots,4$ around the four sets of positions $p_i \approx 1/f_i$.

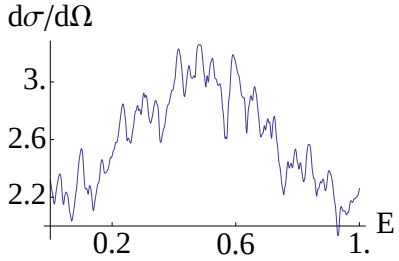

FIGURE 2. Simulated cross section in arbitrary units and power spectrum (right). The abscissa of the cross section is the unit energy interval.

Formally it reads

$$r_k = \sum_{i=1}^{4} h_{i,k}, \quad h_{i,k} = s \sum_{j=1}^{f_i} \frac{\gamma_i^2}{(\frac{k}{300} - j \cdot p_i)^2 + \gamma_i^2} \tag{6}$$

with an overall strength $s = 10^{-5}$. This order of magnitude is based on the mean value of the widths of the compound states being about 10^{-4} to 10^{-5} times smaller than the $\Gamma^{\downarrow}(\gamma_i)$.

The poles at the complex positions ω_k occur in the lower ω-plane with ω being the energy variable. If only $i = 1$ was to occur with $f_1 = 5$, a typical pattern of the residues $h_{1,k}$ is illustrated by the top of Fig.1; similarly for $f_2 = 10$ with $h_{2,k}$ being illustrated by the bottom of Fig.1. The inclusion of further terms would simply add additional peaks to the pattern. In the case presented below we have chosen $f_3 = 16$ and $f_4 = 28$ totalling to 5+10+16+28 additional peaks (not easily visualised, but beautifully discernible in the final analysis). We stress again that the four values f_i were chosen for demonstration purposes and that more than four - or other values - are equally suitable.

These arbitrary numbers used in the example chosen describe particular fragmentations of the QR into altogether 5, 10, 16 and 28 states of increasing complexity. The widths γ_i giving rise to the Lorentzian shape of the residues are in reality determined by the product of the density of the compound states and the coupling of the i-th group to the compound states. The widths are the spreading widths of the respective states considered [15]. As the complexity increases with label i we shall assume $\gamma_1 > \gamma_2 > \gamma_3 > \gamma_4$. In the simulation we endow each γ_i with a random fluctuation with mean value $\gamma_i/4$. As stated above we refrain from specifying a microscopic structure causing the residue pattern assumed for the self-energy; below it becomes clear that guidance comes from experiment.

We also assume that each set f_i is uniformly distributed over the whole energy interval. This is similar in spirit to the assumption used in the local scaling dimension approach [6]. The positions p_i in Eq.(6) are set to be $\sim 1/f_i$ which spreads the actual $j \cdot p_i$ positions equidistantly over the whole interval with j running from 1 to f_i; however, we endow them with a small random fluctuation with mean value $p_i/8$. Note that the random fluctuation of widths and positions generate a mild degree of asymmetry in the energy interval [0,1], resulting in slightly different patterns in the intervals [0,0.5] and [0.5,1]. The near equality of the positions, that is - apart from slight random fluctuations

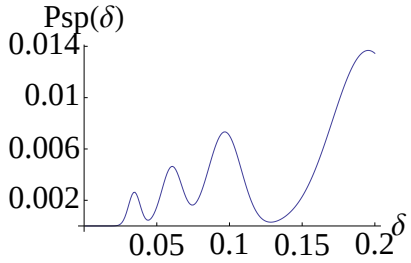

FIGURE 3. Power spectrum from the cross section in Fig 2. The energy values δ refer to the wavelet parameters.

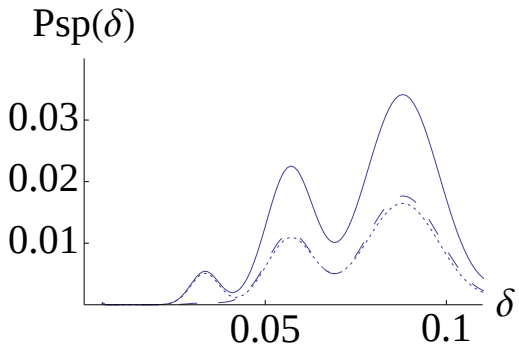

FIGURE 4. Power spectrum for a particular asymmetric situation discussed in text. The dotted curve originates from a scan of the interval [0,0.5], the dashed curve from [0.5,1] and the solid curve from the total interval. Note that the peak on the far left is virtually absent in the dashed curve while fully present in the dotted curve. Units as in Fig.2 and 3.

- the regular pattern of the various fragments as illustrated in Fig.1, is basically dictated by experimental findings: *if there is no near regular pattern there will be no discernible structure in the power spectrum of the wavelet analysis*. However, we shall return below to the case where regular patterns may occur only in a smaller portion of the interval.

The first obvious choice for the widths assumes simply $\gamma_i = 1/(2f_i)$ yielding the simulated cross section shown in Fig.2 (below a precise analytic expression confirming the $1/(2f_i)$-law is given). A variation of such a choice is rather significant, we shall return to this aspect in detail.

THE WAVELET ANALYSIS

The analysis using a Morlet-type mother wavelet

$$\Psi(\omega,\delta) = \frac{1}{\sqrt{\delta}} \cos\frac{k(\omega-\omega_0)}{\delta} \exp -\frac{(\omega-\omega_0)^2}{2\delta^2} \tag{7}$$

is used to calculate the coefficients

$$C(\delta,\omega_0) = \int \frac{\mathrm{d}\sigma(\omega)}{\mathrm{d}\Omega}\Psi(\omega,\delta)\,\mathrm{d}\omega \tag{8}$$

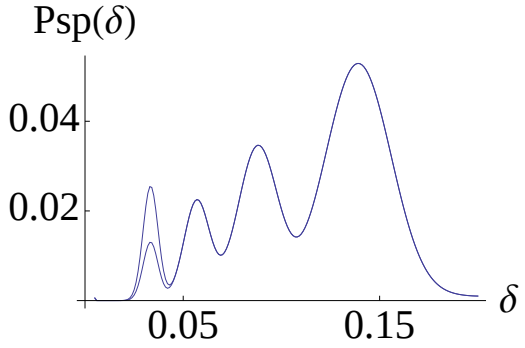

FIGURE 5. Power spectrum: dependence of height at the maximum on spreading width. The curve with the lower value of the most left maximum is identical to the one in Fig.3., while the higher peak is due to a decrease of its spreading width or an increase of its life time. Units as in Fig.2 and 3.

from which the power spectrum

$$Psp(\delta) = \int |C(\delta, \omega_0)|^2 \, \mathrm{d}\omega_0$$

is obtained as a function of the scaling parameter δ. It is shown in Fig.3; if not indicated otherwise we use the value $k = 6$ for the wave number of the mother wavelet. There is in fact a k-dependence of the positions of the maxima of the power spectrum which is given in analytic terms below. A contour plot of $C(\delta, \omega_0)$ is illustrated in Fig.6.

In Fig.3 we clearly discern the four maxima that are produced by the four different values f_i of the number of fragmentations. In fact, the fragmentation into $f_1 = 5$ produces (for $k = 6$) the maximum at $\delta_1^{\max} = 1/f_1 = 0.2$; similarly, the other three maxima occur at $\delta_i^{\max} = 1/f_i$, $i = 2,3,4$. This is one of our major findings:
the maxima of the power spectrum occur at

$$\delta_i^{\max} \approx k/(2\pi) \cdot I/f_i$$

with I being the interval of the whole range of the QR considered and f_i the number of fragmentations. The factor $k/(2\pi)$ originates from the analytic expression given in (7) below. Here we note that this result does not depend on whether we use a real wavelet as in Eq.(7) or its complex version where the cosine-function is replaced by its complex counterpart $\cos(.) + i\sin(.)$.

The asymmetry found in some experimental data can obviously be accounted for by our analysis. We refer to cases where the analysis yields a pattern in the first half of the whole resonance being different from that in the second half, or in principle for any subdivision of the whole resonance. For illustration, we take $f_4 = 14$ while leaving all other parameters unchanged. In this way the total of 28 maxima of the residues r_{f_4} are confined to only 14 within the left half of the interval. The effects are clearly seen in Fig.4. Note that the positions of the maxima still remain unchanged. This type of asymmetry is clearly discernible in Fig.9 of Ref.[10]: from the two-dimensional wavelet transform the wavelet power would give a similarly different pattern when taken at different portions of the whole interval.

The folding (integration) of the cross section with the Morlet wavelet has to be done numerically. In order to obtain an analytic expression relating the number of fragmentations f_i to the positions of the maxima of the power spectrum, we consider an expansion of a cross section into a Fourier series

$$\frac{\mathrm{d}\sigma(\omega)}{\mathrm{d}\Omega} = \sum_m c_m \sin(m\pi\omega/I) + \sum_m c'_m \cos(m\pi\omega/I). \tag{9}$$

An intermediate structure manifests itself, if a few terms in Eq.(9) are appreciably stronger than the others. For Fig.2 the terms with $c_{10} \approx c_{20} \approx c_{32} \approx c_{56}$ (and similarly for the primed coefficients) are dominant; of course, terms for different m-values also occur but are smaller by roughly an order of magnitude or more (here our analysis does not focus on $m \leq 4$: while giving larger contributions such values would correspond to $\delta \geq 0.5$ and represent gross and bulk structure). Performing analytically the wavelet-transform of each term in Eq.(9) (see Appendix), one obtains an analytic evaluation of the positions and heights of the maxima of the power spectrum. For each $\sin(m\pi x)-$ or $\cos(m\pi x)-$term the positions of the local maxima in the power spectrum turn out to be

$$\mathrm{Max}_m = \frac{k+\sqrt{2+k^2}}{2m\pi} I. \tag{10}$$

For $k = 6$ (and the unity interval I) this yields 0.2, 0.1, 0.0625 and 0.036 for $m = 10, 20, 32$ and 56, respectively, as verified in Fig.3. Note that a different choice of k moves the positions of the local maxima, yet the $\sim 1/m$ law prevails. The expression (10) provides an obvious tool to be used to ascertain the number of fragmentations when the maxima are determined from an analysis of experimental data. Clearly, the number f_m of fragmentations introduced above is related to the value m in Eq.(9) by $m = 2f_m$.

Furthermore, an increased value of k can resolve a peak in the power spectrum that is caused by two near values of f_i. In fact, the distance between adjacent maxima (say $m = 17$ and $m = 18$) roughly doubles when k is doubled.

While - for fixed k - the $1/f_i$ dependence of the maxima of the power spectrum is an important finding, even more significant is the result that the values at the maxima (the heights) also obey the same $1/f_i$-law *if the corresponding Fourier coefficients are about equal*. Indeed, a straight line can be drawn through the maxima in Fig.3 since the four values $c_m, m = 10, 20, 32, 56$ are about equal. We recall that, for example, $\sin(10\pi x)$ generates $f_k = 5$ peaks of a width $\gamma_k = 1/(2f_k)$ in the energy (unit) interval for the cross section. This can be exploited in a realistic analysis: a deviation from this straight-line-rule signals effectively a deviation from the spreading width being assumed to be $1/(2f_i)$. This is illustrated in Fig.4 where the spreading width $1/(2f_4)$ has been decreased to $1/(2.8f_4)$. As a result, the value of the first peak becomes enhanced. Since the spreading width is related to the life time of the states, we conclude: *the life times are proportional to f_i if the heights of the maxima lie on a straight line; an increased (decreased) height signals an even longer (shorter) life time.*

In this context we note that the *number* of peaks and troughs in Fig.5 on the horizontal lines matches exactly the values of the f_i: five on the top, further down ten, then sixteen and twenty eight on the bottom. The actual values of these peaks and troughs determine the heights of the bumps in the power spectrum, that is the information about the life

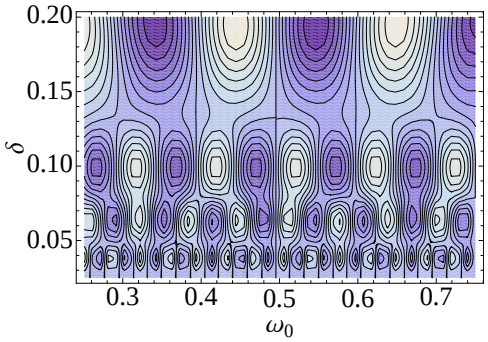

FIGURE 6. Wavelet contour plot of cross section shown in Fig.3. The symbols δ and ω_0 refer to the Morlet wavelet parameters used in Eq.(7). The (positive) maxima are in light shading and the (negative) minima in dark. For the top pattern the contours range from 0.4 to -0.4.

times of the respective fragmented states. A similar wavelet transform obtained from experimental data is presented in Figs.8 and 9 in Ref.[10]; note that our schematic 'in vitro' illustration is of course much more symmetric.

CONCLUSION

While in experiments the chaotic nature of the nucleus usually shows at higher excitation energies [16], the pertinent structure revealed in the analysis may come as a surprise. We are of course familiar with order in the nuclear many body system as shown in shell effects and simple collective states. The fragmentations of the QR may be due to a different quality: it could be a manifestation of *self-organising structures* [18, 19, 20]. Indeed, the life time of increasingly complex configurations of the QR is increasing toward the compound states and the ground state. There is no generally accepted definition of conditions under which the self-organising structures are expected to arise. We may speculate that in the case considered here, once the nuclear QR state is created, it is driven to an unstable hierarchy of configurations (metastable states) by quantum selection rules which connect these different complex configurations due to internal mixing. This problem needs of course a dedicated study on its own and is beyond the scope of the present paper.

We summarise the major points of our findings: (i) the position of the peaks in the power spectrum indicate the number of fragmentations of a particular intermediate state; the more complex states lie to the left of the simpler states (see Eq.(10)); (ii) the resolution of poorly resolved peaks can be improved by a higher value of k; (iii) the values (heights) at the peaks are related to the spreading widths, implying knowledge about the life times: if they lie on a straight line, the life times are proportional to the number of fragmentations, if they lie above (below) the straight line the corresponding life times are longer (shorter). Finally, we mention that a pronounced gross structure of the experimental cross section as found in lighter nuclei, would have no effect upon our findings. In fact, such gross structure had to occur at the far right end (values of δ appreciably larger than those used in the literature) of the power spectrum.

APPENDIX

The wavelet transform of each term in Eq.(9) is for the $\sin m\pi\omega$-term (with $m\pi = a$)

$$\frac{1}{\sqrt{\delta}}\int_0^1 \mathrm{d}x \sin ax \cos\frac{k(x-\varepsilon)}{\delta}\exp-\frac{(x-\varepsilon)^2}{2\delta^2} = -\sqrt{\frac{\pi}{2}}\frac{\sqrt{\delta}}{2}\exp(-\frac{(a\delta+k)^2}{2})\cdot$$
$$\Im(\exp(-ia\varepsilon)\mathrm{Erf}\frac{1+ia\delta^2-\varepsilon+i\delta k}{\sqrt{2}\delta}) + \Im(\exp(-ia\varepsilon+2a\delta k)\mathrm{Erf}\frac{1+ia\delta^2-\varepsilon-i\delta k}{\sqrt{2}\delta})$$
$$+\Im(\exp(ia\varepsilon)\mathrm{Erf}\frac{-ia\delta^2-\varepsilon-i\delta k}{\sqrt{2}\delta}) + \Im(\exp(ia\varepsilon+2a\delta k)\mathrm{Erf}\frac{-ia\delta^2-\varepsilon+i\delta k}{\sqrt{2}\delta})$$

and similar for the $\cos m\pi\omega$-term where the $\Im$ is replaced by $\Re$. Here Erf denotes the error function. The positions of the maxima in Fig 3 are the zeros of the derivative with respect to δ of the square of the expression above (we assume that the maxima are isolated). This amounts to finding the zeros of the derivative. The derivative reads

$$\begin{aligned}
&\frac{-1+\exp(2ia\varepsilon)}{16\delta^{3/2}}\Big\{ i\sqrt{2\pi}\delta\exp(-\frac{k^2+a^2\delta^2+2ia\varepsilon}{2}) \\
&\Big(\exp(ak\delta)(-1+2a\delta(-k+a\delta))\Im\mathrm{Erf}(\frac{\varepsilon+i\delta(k-a\delta)}{\sqrt{2}\delta}) \\
+\;& \exp(-ak\delta)(-1+2a\delta(k+a\delta))\Im\mathrm{Erf}(\frac{\varepsilon-i\delta(k+a\delta)}{\sqrt{2}\delta})\Big) \\
-\;& 4\exp(-\frac{\varepsilon(\varepsilon+2i\delta(k+2a\delta))}{2\delta^2})(1+\exp(\frac{2i\varepsilon k}{\delta})(-i(1+\exp(2ia\varepsilon))\varepsilon \\
+\;& a(-1+\exp(2ia\varepsilon))\delta^2\Big\}.
\end{aligned}$$

This expression has three terms: two within the big round brackets and a third before the closing curly bracket. For the parameter range of interest, owing to the exponential factors only the first term within the round brackets contributes substantially while the other two terms are smaller by many orders of magnitude. This first term, in turn, is governed by the factor $(-1+2a\delta(-k+a\delta))$. It vanishes, and thus the whole expression, for $\delta = (k+\sqrt{2+k^2})/(2a) = (k+\sqrt{2+k^2})/(2m\pi)$ being the expression given in Eq.(10).

ACKNOWLEDGMENTS

WDH is thankful for the hospitality which he received from the Nuclear Theory Section of the Bogoliubov Laboratory, JINR during his visit to Dubna. The authors gratefully acknowledge enlightening discussions with J. Carter, R. Fearick and P. von Neumann-Cosel. This work is partly supported by JINR-SA Agreement on scientific collaboration, by Grant No. FIS2008-00781/FIS (Spain) and RFBR Grants No. 08-02-00118 (Russia).

REFERENCES

1. M. N. Harakeh and A. van der Woude, *Giant Resonances: Fundamental High-Frequency Modes of Nuclear Excitation* Clarendon Press, Oxford, 2001.
2. A. Bohr and B. R. Mottelson, *Nuclear Structure*, v.II World Scientific, Singapore, 1998.
3. P. Ring and P. Schuck, *The Nuclear Many-Body Problem* Springer-Verlag, New York, 1980.
4. R. Lauritzen, F. P. Bortignon, R. A. Broglia, and V. G. Zelevinsky, *Phys. Rev. Letters* **74**, 5190 (1995).
5. V. V. Sokolov and V. G. Zelevinsky, *Phys. Rev. C***56**, 311 (1997).
6. H. Aiba and M. Matsuo, *Phys. Rev. C***60**, 034307 (1999).
7. D. Lacroix and P. Chomaz, *Phys. Rev. C***60**, 064307 (1999).
8. A. Shevchenko, J. Carter, R. W. Fearick, S. V. Förtsch, H. Fujita, Y. Fujita, Y. Kalmykov, D. Lacroix, J. J. Lawrie, P. von Neumann-Cosel, R. Neveling, V. Yu. Ponomarev, A. Richter, E. Sideras-Haddad, F. D. Smit, and J. Wambach, *Phys. Rev. Letters* **93**, 122501 (2004).
9. A. Shevchenko, G. R. J. Cooper, J. Carter, R. W. Fearick, Y. Kalmykov, P. von Neumann-Cosel, V. Yu. Ponomarev, A. Richter, I. Usman and J. Wambach, *Phys. Rev. C* **77**, 024302 (2008).
10. A. Shevchenko, O. Burda, J. Carter, G. R. J. Cooper, R. W. Fearick, S. V. Förtsch, Y. Fujita, Y. Kalmykov, D. Lacroix, J. J. Lawrie, P. von Neumann-Cosel, R. Neveling, V. Yu. Ponomarev, A. Richter, E. Sideras-Haddad, F. D. Smit, and J. Wambach, *Phys. Rev. C* **79**, 044305 (2009).
11. I. Daubechies, *Ten Lectures on Wavelets*, SIAM, Vol.**61** (1992).
12. S. Mallat, *A Wavelet Tour of Signal Processing* Academic Press, San Diego, 1998.
13. H. L. Resnikoff and R. O. Wells Jr., *Wavelet Analysis: The Scalable Structure of Information* Springer-Verlag, New York, 2002.
14. J.-P. Blaizot and G. Ripka, *Quantum Theory of Finite Systems* The MIT Press, London, 1986.
15. F. J. W. Hahne and W. D. Heiss, *Ann. Physics* **89**, 68 (1975).
16. T. Guhr, A. Müller-Groeling, and H. Weidenmüller, Phys. Rep. **299**, 189 (1998); H. A. Weidenmüller and G. E. Mitchell, *Rev. Mod. Physics* **81**, 539 (2009).
17. C. L. Bai, H. O. Zhang, X. Z. Zhang, F. R. Xu, H. Sagawa, and G. Coló, *Phys. Rev. C* **79**, 041301(R) (2009).
18. P. Bak, C. Tang, and K.Wiesenfeld, *Phys. Rev. Letters* **59**, 381 (1987).
19. H. J. Jensen, *Self-Organized Criticality: Emergent Complex Behaviour in Physical and Biological Systems* Cambridge University Press, Cambridge, 1998.
20. D. Sornette, *Critical Phenomena in Natural Sciences. Chaos, Fractals, Selforganization and Disorder: Concepts and Tools* Springer, Berlin, 2000.